

**UCC Library and UCC researchers have made this item openly available.
Please [let us know](#) how this has helped you. Thanks!**

Title	AC-assisted single-nanowire electromechanical switch
Author(s)	Andzane, Jana; Meija, Raimonds; Livshits, Alexander I.; Prikulis, Juris; Biswas, Subhajit; Holmes, Justin D.; Erts, Donats
Publication date	2013-09-10
Original citation	Andzane, J., Meija, R., Livshits, A. I., Prikulis, J., Biswas, S., Holmes, J. D. and Erts, D. (2013) 'An AC-assisted single-nanowire electromechanical switch', Journal of Materials Chemistry C, 1(43), pp. 7134-7138. doi: 10.1039/c3tc31240b
Type of publication	Article (peer-reviewed)
Link to publisher's version	http://pubs.rsc.org/en/content/articlelanding/2013/tc/c3tc31240b http://dx.doi.org/10.1039/c3tc31240b Access to the full text of the published version may require a subscription.
Rights	© Royal Society of Chemistry 2013
Item downloaded from	http://hdl.handle.net/10468/6698

Downloaded on 2022-11-28T11:11:57Z

Cite this: DOI: 10.1039/c0xx00000x

FULL PAPER

www.rsc.org/xxxxxx

AC-Assisted Single-Nanowire Electromechanical Switch

Jana Andzane,^{*a} Raimonds Meija,^a Alexander I. Livshits,^a Juris Prikulis,^a Subhajit Biswas,^{b,c}, Justin D. Holmes^{b,c} and Donats Erts^a

Received (in XXX, XXX) Xth XXXXXXXXXX 20XX, Accepted Xth XXXXXXXXXX 20XX

DOI: 10.1039/b000000x

A unique two-source controlled nanoelectromechanical switch has been assembled from individual, single-clamped Ge nanowires. The switching behaviour was achieved by superimposing control signals of specific frequencies to the electrostatic potential of the output terminals, eliminating the need for an additional gate electrode. Using an *in-situ* manipulation technique inside a scanning electron microscope, we demonstrate that the pull-out force required to overcome adhesion at contact can be significantly reduced by exciting mechanical resonant modes within the nanowire.

Introduction

Nanoelectromechanical systems (NEMS) are devices which integrate electrical and mechanical functionality at the nanoscale and are the obvious next step in the miniaturisation of microelectromechanical systems (MEMS).¹ NEMS potentially exhibit a range of properties that could significantly impact many areas of technology and science, complementing or replacing current MEMS. The expected benefits of NEMS over MEMS include higher efficiencies, reduced size, decreased power consumption and lower production costs.²

Current examples of NEMS include a range of nanorelays and switches (ON-OFF devices),^{3-10,12-17} Carbon nanotubes as well as metal and semiconductor nanowires have been used as active components in such devices.^{1, 3-10} In particular, single crystalline nanowires are excellent candidates for NEMS due to their uniform chemical structure and improved mechanical properties, low mass and good structural and compositional reproducibility.¹⁸ Most electrically controlled ON-OFF devices utilise three electrodes, namely source, drain and gate. The gate potential in a typical NEMS switch induces a polarisation charge in the active nanowire element resulting in an electrostatic force,^{3-5, 16,17} which changes the mechanical configuration of the device. The ON-OFF switching of NEMS can also be achieved in a gateless two-terminal configuration, which has been investigated both theoretically^{19,20} and experimentally.^{3,5,6,9-11,12,16,17,21-13} The advantage of such devices in comparison to gated NEMS is the simplicity of implementation, where only two electrodes, drain and source are used.

The basic operating principle underlying gateless switching of NEMS is the interplay of electrostatic, adhesion and elastic energies. Detailed descriptions of one- and two-source gateless switches were presented recently by our groups.²⁴ However the reported two-source gateless NEMS, based on the elastic forces

between the active element and the contact, has two main drawbacks: (i) the detachment of the active element from a contact depends on the ‘pull-off’ elastic force, *i.e.* the physical properties of the nanowire and the distance between the nanowire and the source electrode. This distance should be large enough to achieve the necessary force required to detach the nanowire from contact when necessary, without causing a large fluctuation of the jump-to-contact voltage. (ii) Static gateless devices become unreliable in the ON state due to unwanted disconnection, which limits device configuration and the low operating voltage range employed.

In this paper, an *in-situ* investigation of the pull-out mechanisms in two-source Ge nanowire nanoelectromechanical switches is presented. The key feature of these devices is that nanowire pull-off is assisted by the excitation of mechanical resonant modes in the switching element. The switching of the active element between the two sources is fully controllable by manipulating the elastic force of Ge nanowires and both DC and AC electric fields. Most notably, the operating voltages employed are much lower compared to static-only nanoelectromechanical switching devices.

Experiment

Ge nanowires used as active elements were synthesised using a supercritical fluid-liquid-solid (SFLS) approach.⁹ Ge nanowires were grown in 5 ml stainless steel cell (High Pressure Equipment Company) at a temperature of 400 °C. The handling of dry toluene and diphenylgermane (Ge precursor), as well as the filling of the reaction vessel and injection cell was carried out in a N₂ glove box under stringent precautions against water. In a typical experiment Au nanoparticle solutions were spin coated onto a Si(001) substrate and loaded into the reaction cell. The reaction cell and injection equipment were dried under vacuum at 180 °C for 48 h and transferred into the glove box. 3 ml toluene

was added to the reaction cell and the assembly was heated to the desired temperature in a tube furnace for 2 h. After setting the pressure of the reaction cell to 21 MPa, the injection cell, filled with 20 ml of toluene/diphenylgermane solution ($2.5 \mu\text{mol ml}^{-1}$), was set to the identical pressure by an ISCO high pressure pump. The precursor solution was injected at a rate of $0.025 \text{ ml min}^{-1}$ over a time period of 120 min under constant pressure conditions in a flow through reaction. Finally, the reaction cell was cooled to room temperature, depressurised and disassembled to access the growth substrate. Nanowires were washed with dry toluene and dried under a flow of N_2 .

The lengths of the nanowires used in these experiments ranged from between 15–110 μm , with radii dimensions between 50–100 nm. A 13D SmarAct nanopositioners inside a Hitachi FE-4800 scanning electron microscope (SEM) was used for process visualisation and nanowire-electrode distance adjustments. The nanopositioner system allows adjustment of the electrode and nanowire positions, without the need for lithographic processing.

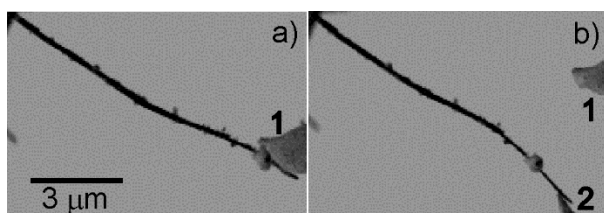


Fig. 1. SEM images of (a) a Ge nanowire in contact with electrode 1 and (b) the same Ge nanowire switched from the electrode 1 to electrode 2.

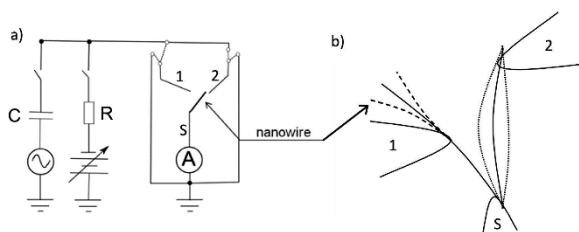


Fig. 2. (a) Schematic of the experiment set-up for reduced DC switching. The DC and AC fields can be applied between the selected source electrode and the nanowire tip separately or together. (b) Modes of the nanowire oscillation between electrodes 1, 2 and S.

Ge nanowires were attached to the sharp Au tips (sample tips) as follows: Au tips are prepared by electrochemical etching of 0.25 mm 99.99 % Au wire in 20 % hydrochloric acid at an applied voltage of 5.5–6.5 V. For the electrochemical etching, a Park Scientific Instruments TE-100 STM TIP ETCHER was used. The apex of the etched Au tip was carefully immersed in the conductive epoxy CW2400 and left to dry for 15 min. The epoxy containing apex of the Au tip was then brought in contact with the Ge nanowires and slowly withdrawn. A number of nanowires remained glued to the tip apex. This process was visualized under a $8 \times$ optical microscope using a 3D mechanical manipulator. A Keithley-6430 Source Meter was used for electric measurements. An additional resistance of 100 M Ω was connected in series as a current limiter.

For the device configuration, Au electrodes and sample tip containing Ge nanowires were attached to the manipulators of 13D SmarAct nanopositioners, which was subsequently placed inside an SEM and electrically connected. Initially, all electrodes

and the sample tip were grounded. The electrodes and sample tip were moved to desired positions manually using the nanopositioners. The minimal step of the nanopositioner was 50 nm, which was enough for the fine adjustment of the device configuration. When all of the electrodes and the sample tip were brought to the desired positions, the appropriate voltages were applied to induce nanowire switching. The positions of the electrodes and the sample tip could be adjusted using the nanomanipulator as necessary.

Results and Discussion

Figure 1 shows SEM images of a Ge nanowire switching device which operates using a ‘static only’ electric field. The Ge nanowire shown in figure 1(a), and in contact with electrode 1, has a length of 13 μm and a radius of 50 nm. The distance between electrodes 1 and 2 shown in figure 1(b) is 3 μm . Switching of the Ge nanowire from electrode 1 to 2 occurred upon application of a DC voltage (180 V) between electrode 2 (source) and the nanowire tip. Quantitatively the ‘static only’ system can be characterised by the following approximate values: the adhesion force between the nanowire and electrode 1, based on a contact area of 965 nm^2 was calculated by Carpick’s generalised equation^{25,26} to be around 500 nN. The elastic force of the bent Ge nanowire, calculated using a Young’s modulus value for bulk Ge of 103 GPa, was found to be close to 45 nN, which is an order of magnitude smaller than the adhesion force. The electrostatic force between electrode 2 and the Ge nanowire, calculated using a sphere-plane geometry²⁷ and corresponding to an applied pull-off voltage equals 480 nN, which together with the elastic force is sufficient to overcome the adhesion between the nanowire and electrode 1 and trigger switching. Figure 2 shows schematically how an additional AC component can be used to reduce the DC fields required for switching the nanowires. The control voltage is formed using a simple RC network as shown in figure 2(a). The AC component supplies the nanowire with additional energy by exciting resonant modes within its structure (figure 2(b)), at frequencies dependent on the geometry of the nanowire. This extra kinetic energy can assist the nanowire to escape the attractive potential of the contact at conditions which would make pull-off impossible using DC fields only.

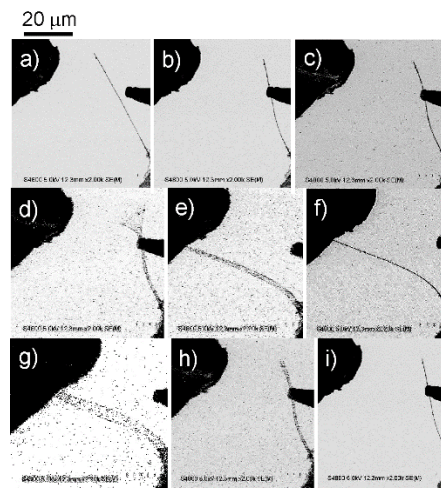


Fig. 3. (a) to (i) SEM images of the step-by-step operation of a two-source nanowire switch controlled by combined DC-AC fields.

For repetitive back and forth switching, one of the electrodes should be located near the middle of the nanowire, while the other near its end. In such a configuration the resonance frequencies of the indicated modes will be similar or ideally equal, as discussed later in this article. To detach the nanowire from electrode 1, the AC field can be added to the DC field between electrodes 2 and S. By sweeping the AC field frequency, the free end of the nanowire can be excited at its resonance frequency (dashed lines) (figure 2(b)). This excitation will provide additional energy to the nanowire, resulting in successful disconnection at reasonable DC voltages. To detach the nanowire from the electrode 2, an AC field should be applied between electrodes 1 and S on top of the DC field; exciting the double-clamped mode at its resonance frequency to achieve disconnection (point lines).

Figure 3 shows a sequence of SEM images of an operating two-source nanowire switch, controlled by a combined DC-AC

field. The length and the radius of the Ge nanowire was $40\ \mu\text{m}$ and $60\ \text{nm}$ respectively. The distance between the two source electrodes was $17\ \mu\text{m}$. The Ge nanowire initially started in a neutral position between the two source electrodes (figure 3(a)). A DC field sweep was slowly applied between electrode 2 and the sample tip. At $7\ \text{V}$ the nanowire jumped to electrode 2 (figure 3(b)). Contact with the electrode occurred near the middle of the nanowire. After contact, both electrode 2 and the tip of the nanowire were switched to ground and a $15\ \text{V}$ DC potential was applied between the nanowire and electrode 1, resulting in a slight bending of the nanowire towards electrode 1 (figure 3(c)). After the nanowire was slightly bent, an AC field with $4\ \text{V}$ amplitude was added to the $15\ \text{V}$ DC field and the resonant frequency of the free end of the nanowire was determined. For the particular configuration shown in figure 3, the resonance frequency of the Ge nanowire was found to be approximately $235\ \text{kHz}$ (figures 2(b) and 3(d)). When the AC amplitude was increased to $6\ \text{V}$, the nanowire switched from electrode 2 to

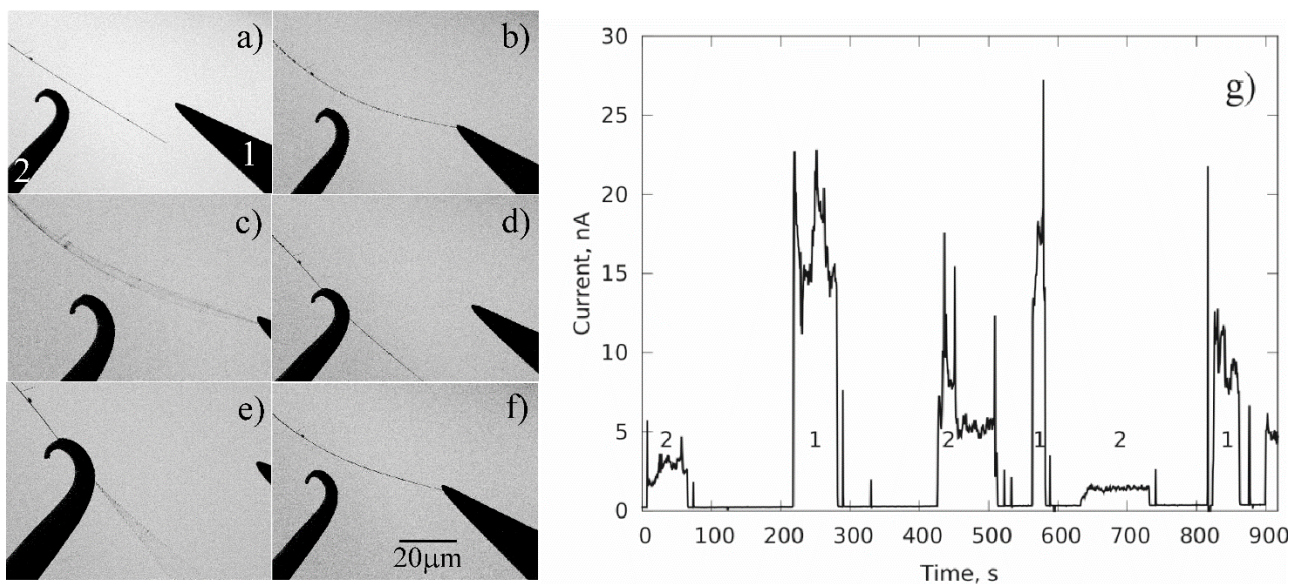


Fig. 4. Operation of a DC-AC field controlled nanowire switch. The operational DC field was $20\ \text{V}$: (a) the initial position of the nanowire between the source electrodes; (b) the nanowire in contact with the electrode 1; (c) the double-clamped nanowire is resonating under the influence of AC field. The AC amplitude is $2.75\ \text{V}$; (d) the nanowire switches to electrode 2 at an AC amplitude of $12.5\ \text{V}$; (e) the free end of the nanowire is resonating under the influence of AC field. AC amplitude is $1\ \text{V}$; (f) the nanowire switches to electrode 1 at AC amplitude of $10\ \text{V}$; (g) the current-time characteristics of the device. Current jumps are labeled with numbers of source electrode with which contact occurred.

Cite this: DOI: 10.1039/c0xx00000x

FULL PAPER

www.rsc.org/xxxxxx

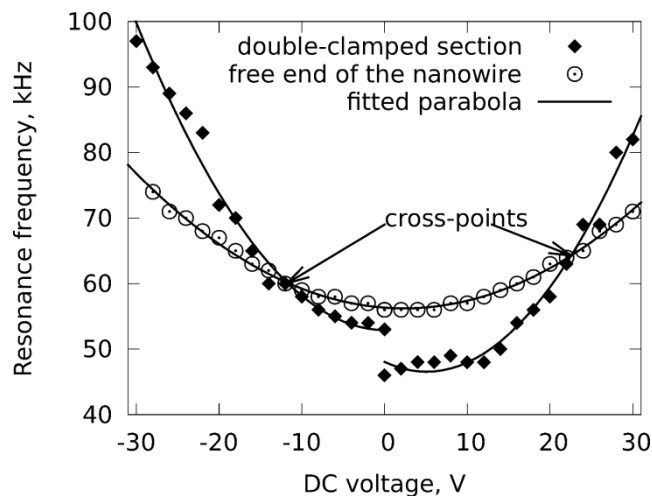


Fig. 5. Dependence of the resonant frequency of a Ge nanowire on the DC field applied between electrodes.

electrode 1 (figure 3(e)).

For the reverse switching, the nanowire in contact with electrode 1 was connected to ground and a 15 V DC field was applied to electrode 2; a slight bending of the nanowire towards electrode 2 was observed (figure 3(f)). An AC field of 12 V was subsequently added alongside the DC field. The resonant frequency of the double-clamped Ge nanowire for the particular configuration shown in figure 3 was found to be 273 kHz (figures 2(b) and 3(g)). When the AC amplitude was increased to 14 V, the nanowire switched to electrode 2, as shown in figure 3(h). Afterwards, both DC and AC fields were turned off and the switching cycle was repeated (figure 3(i)). In order to emphasise the efficiency of AC-assisted switching, the distance between the source electrodes was chosen to be much larger than was the case for the DC-only experiment shown in figure 1, *i.e.* 17–30 μm versus 3 μm respectively. The estimated equivalent DC voltage required for the nanowire switching at a distance of 17 μm would exceed 380 V, which is unreasonable for the operation of a practical device.

The reliability of repetitive operation of the AC-assisted switch is demonstrated in figure 4. In this example, the nanowire switch operated at a constant DC voltage of 20 V and an AC amplitude of 10–12 V. The length and radius of the nanowire was 110 μm and 50 nm respectively. In the experiment, the resonant frequency varied between 87–91 kHz for the double-clamped nanowire (figures 4(b) (c)) and between 58–61 kHz for the free end of the nanowire (figures 4(d) and (e)). The resonant frequencies were dependent on the contact conditions, which may differ each time the contact geometry is changed. However, for application in practical devices this problem may be addressed by a more rigid and compact design.

Current jumps of up to 20 nA were registered every time the

nanowire made contact with one of the source electrodes. Contact with electrode 2 occurred near the middle of the nanowire. Contact with the electrode 1 occurred near the end of the nanowire. During contact with electrode 1, the effective length of the nanowire and consequently its electric resistance, was approximately two times smaller than when the nanowire was in contact with electrode 1. Hence higher currents were registered through the electrode 1, as shown in figure 4(g).

The application of AC assisted-gateless switches in practical devices would require operation in both directions using a single, fixed frequency source. Gateless switching is possible by balancing the frequencies of the double clamped and single clamped modes through geometric alignment of the source electrodes. Additional tuning of the frequency is possible by varying the applied electrostatic field. Figure 5 shows the resonance frequency dependence of a nanowire based on the DC voltage applied between two electrodes, using the same electrical circuit as shown in figure 1(a) and for both modes of the nanowire switch as shown in figure 4. During the experiment the DC voltage was increased from zero to ± 30 V, but the nanowire was connected either to electrode 1, or to electrode 2. On one occasion, when the nanowire was connected to electrode 2 and a potential of 30 V was reached, disconnection occurred. As a result, the nanowire had to be brought into contact again before the experiment could be continued at negative voltages. Slight changes in the contact geometry sometimes caused a discontinuity at 0 V, as shown on the graph. Nevertheless, each branch of the collected data fits well with parabolic equations. The external electrical field adds tension to the nanowire and hence the resonance frequency increases. Notably the minimum frequency appears at slightly positive voltages, probably due to the build-up of negative charge on the oxidised surface of the nanowire caused by the SEM electron beam. Although the exact DC offset for a frequency minimum cannot be accurately measured due to experimental drift, similar asymmetry of positive and negative branches has been observed in a number of our experiments. The key observation from figure 5 is that the recorded frequency-voltage lines cross and a DC voltage can be found for which both oscillation modes have the same frequency. This dependence has been measured at reduced AC signal levels in order not to cause switching. For normal operation the AC signal should be increased above a certain threshold, which for the device shown in figure 4 is approximately 10 V.

An estimate of the switching speeds can be calculated using a damped oscillator model with a harmonic drive. The settling time (τ) for such a system is inversely proportional to the resonance width ($\Delta\omega$) in the frequency domain. A typical quality factor $Q = \omega_0 / \Delta\omega$ for Ge nanowires used in our experiments was 100–400, where $\omega_0 = 2\pi f_0$ is the resonance frequency. Thus for a 100 kHz oscillator with stationary amplitude moderately exceeding the pull-off threshold, the switching time would be

below 1 ms. Following this simple model, the switching speed can be increased using larger drive amplitudes; however the most significant improvement would be to use shorter nanowires with higher resonance frequencies while maintaining relatively low values of Q .

Conclusions

We have successfully demonstrated a new type of gateless NEMS switching device where resonant oscillation modes of a single nanowire are used to break the adhesion potential of the contact. The voltage levels required to drive such a device are about 10 times smaller compared to equivalent static-only switches, ensuring stable operation of the device and contributing to its durability. Crucial for practical implementation is precise alignment of the electrodes, which determines the geometric conditions of resonant oscillations. We also demonstrate how DC voltages can be used to tune the AC frequency required for the operation. Although Ge nanowires were used in the demonstration, the same method could be applied to other materials. The experiments were done on relatively long nanowires in order to emphasise the efficiency of AC-assisted switching. Further developments to improve the stability and speed of the nanowire switches, through a more compact and rigid design with higher resonance frequencies, is currently in progress.

Acknowledgements

We acknowledge financial support from Council of Science Latvia (Grant Nr.549/2012) and Science Foundation Ireland (Grant: 09/IN.1/I2602)

Notes and references

^a Institute of Chemical Physics, University of Latvia, Riga, Latvia; E-mail: jana.andzane@lu.lv

^b Materials Chemistry & Analysis Group, Department of Chemistry and the Tyndall National Institute, University College Cork, Cork, Ireland

^c Centre for Research on Adaptive Nanostructures & Nanodevices (CRANN), Trinity College Dublin, Dublin 2, Ireland

- 1 P. Kim, C. Lieber, *Science*, 1999, **126**, 2148.
- 2 J.E. Hughes Jr, M. D. Evoy, *Berlin: Springer*, 2004, ISBN1-4020-7720-3.
- 3 O. W. Loh, D. Espinosa, *Nature Nanotechnology*, 2012, **7**, 283-295.
- 4 H. J. Hwang, J. W. Kang, *Physica E*, 2005, **27**, 163.
- 5 Z. Chen, L. Tong, Z. Wu, Z. Liu, *Appl. Phys. Lett.*, 2008, **92**, 103116.
- 6 C. Ke, H. D. Espinosa, *Small*, 2008, **92**, 103116
- 7 T. Rueckes, K. Kim, E. Joslevich, G. Y. Tseng, C.-L. Cheung, C. M. Lieber, *Science*, 2000, **289**, 94.
- 8 J. Kinaret, T. Nord, S. Viefers, *Appl. Phys. Lett.*, 2003, **82**, 1287.
- 9 J. Andzane, N. Petkov, A. Livshits, J. Boland, J. Holmes, D. Erts, *Nano Lett.*, 2009, **9-5**, 1824.
- 10 K. J. Ziegler, D. M. Lyons, J. D. Holmes, D. Erts, B. Polyakov, H. Olin, E. Olsson, K. Svensson, *Appl. Phys. Lett.*, 2004, **84**, 4074.
- 11 X. Q. Li, S. M. Koo, C. A. Richter, M. D. Edelstein, J. E. Bonevich, J. J. Kopanski, J. S. Suehle, E. M. Vogel, *IEEE Trans. Nanotechnol.* 2007, **6**, 256.
- 12 J. Andzane, J. Prikulis, D. Dvorsek, D. Mihailovic, D. Erts, *Nanotechnology*, 2010, **21**, 125706.
- 13 S. Lee, D. Lee, R. Morjan, S. Jhang, M. Svenningsson, O. Nerushev, Y. Park, E. Campbell, *Nano Lett.*, 2004, **4**, 2027.
- 14 V. Viasnoff, A. Meller, H. Isambert, *Nano Lett.*, 2006, **6**, 101.
- 15 J. E. Jang, S. N. Cha, Y. J. Choi, D. J. Kang, T. P. Butle, D. G. Hasko, J. E. Jung, J. M. Kim, G. A. Amaratunga, *Nat. Nanotechnology*, 2008, **3**, 26.

- 16 W. W. Jang, J. O. Lee, J. B. Joon, M. S. Kim, J. M. Lee, S. M. Kim, K. H., Cho, D. W. Kim, D. Park, W. S. Lee, *Appl. Phys. Lett.*, 2008, **92**, 103110.
- 17 J. E. Jang, S. N. Cha, Y. Choi, A. J. Gehan, A. J. Amaratunga, D. J. Kang, H. G. Hasko, J. E. Jung, J. M. Kim, *Appl. Phys. Lett.*, 2005, **87**, 163114.
- 18 H. Li, F. Sun, *Nanowires-Recent Advances*, book edited by Xihong Peng, ISBN 978-953-51-0898-6, 2012, chapter 16.
- 19 M. Dequesnes, S. V. Rotkin, N. R. Aluru, *Nanotechnology*, 2002, **13**, 120.
- 20 K. A. Bulashevich, S. V. Rotkin, *JETP Lett. (Engl. Transl.)*, 2002, **75**, 205
- 21 S. Akita, Y. Nakayama, S. Mizooka, Y. Takano, T. Okawa, Y. Miyatake, S. Yamanaka, S. M. Tsuji, T. Nosaka, *Appl. Phys. Lett.*, 2001, **79**, 1691.
- 22 E. Dujardin, V. Derycke, M. F. Goffman, R. Lefe`vre, J. P. Bourgoin, *Appl. Phys. Lett.*, 2005, **87**, 193107.
- 23 D. Erts, H. Olin, L. Ryen, E. Olsson, A. Thölen, *Phys. Rev. B*, 2000, **12**, 725.
- 24 J. Andzane, J. Prikulis, R. Meija, J. Kosmaca, S. Biswas, J. D. Holmes, D. Erts, *Mater. Sci. (Medžiagotyra)*, 2012, in press.
- 25 R. W. Carpick, D. F. Ogletree, M. Salmeron, *J. Colloid Interface Sci.*, 1999, **211**, 395.
- 26 D. Erts, A. Löhmus, R. Löhmus, H. Olin, A. V. Pokropivny, L. Ryen, K. Svensson, *Appl. Surf. Sci.*, 2002, **188**, 460.
- 27 B. D. Terris, J. E. Stern, D. Rugar, H. J. Mamin, *Phys. Rev. Lett.*, 1989, **63**, 2669.